Rapid synthesis of thermoelectric YB22C2N via spark plasma sintering with gas/solid reaction technology

Hyoung-Won Son, Philipp Sauerschnig, David Berthebaud, Takao Mori

JCS–Japan

EXPRESS LETTER

Rapid synthesis of thermoelectric $YB_{22}C_2N$ via spark plasma sintering with gas/solid reaction technology

Hyoung-Won SON[1,2], Philipp SAUERSCHNIG[1,2], David BERTHEBAUD[3] and Takao MORI[1,2,†]

[1] WPI International Center for Materials Nanoarchitechtonics (WPI-MANA) and Center for Functional Sensor & Actuator (CFSN),
 National Institute for Materials Science (NIMS), 1–1 Namiki, Tsukuba, Ibaraki 305–0044, Japan
[2] Graduate School of Pure and Applied Sciences, University of Tsukuba, 1–1–1 Tennoudai, Tsukuba, Ibaraki 305–8671, Japan
[3] CNRS-Saint Gobain-NIMS, UMI 3629, Laboratory for Innovative Key Materials and Structures (LINK),
 National Institute for Materials Science (NIMS), 1–1 Namiki, Tsukuba, Ibaraki 305–0044, Japan

Dense $YB_{22}C_2N$ samples were directly synthesized from powder mixtures via reactive spark plasma sintering. The gas/solid reaction step was applied to introduce nitrogen into the mixture during heating. The sample reactively sintered at 1700 °C for 10 min after the gas/solid reaction step at 1200 °C for 30 min consisted of $YB_{22}C_2N$ with small amounts of secondary phases. The thermoelectric behavior shifted toward n-type behavior with increasing amount of $YB_{22}C_2N$ phase. This newly developed synthesis technique could facilitate the rapid and cost-effective preparation of complex borocarbonitrides.
©2020 The Ceramic Society of Japan. All rights reserved.

Key-words : Boride, Thermoelectric, Spark plasma sintering, Reactive sintering, Gas/solid reaction, Nitridation

The rare earth borides are a rich class of materials exhibiting interesting structural and physical properties such as superconductivity, magnetism, and thermoelectricity, for example.[1]–[9] The homologous series of rare earth borocarbonitrides; $RB_{15.5}CN$, $RB_{22}C_2N$, $RB_{28.5}C_4$ were found to exhibit unexpectedly strong magnetic coupling for dilute magnetic insulators,[10],[11] and interesting two-dimensional (2D) spin glass-like behavior.[12]–[14] This series of compounds were also found to be the long-awaited thermoelectric n-type counterpart to boron carbide.[15]–[17]

Despite the attractive properties, the synthesis of these compounds has always been noted to be difficult, necessitating a complex and time consuming process (≥9 steps; ≥4 days) involving long-time sintering (≥10 h), typically multiple re-sintering, crushing and washing processes.[10],[18]–[20] Densification of the material was also found to be difficult, with initial spark plasma sintering (SPS) experiments only yielding a maximum ~75% density.[16] Several sintering aids were found to lead to highly densified samples, but these additives were found to be detrimental to the thermoelectric properties.[19],[20]

In this study, we report on the first attempt of direct synthesis of complex borocarbonitrides through reactive SPS with gas/solid reaction. A new synthesis method for $YB_{22}C_2N$ from raw materials (except N) was developed to shorten the synthesis time and to attain dense samples.

In order to introduce nitrogen into the mixture and to help the formation of the objective phase, gas/solid reaction technology was used during the heating process. Such in situ nitridation during SPS has already been reported for titanium alloy-based composites,[21] but to our knowledge, this is the first example of direct nitride synthesis of borocarbonitrides through reactive SPS.

Commercially available YB_4 (99.9%, Japan New Metals Co., Ltd.), amorphous B (99%, New Metals and Chemicals Co., Ltd.) and graphite (Sigma-Aldrich Co., Ltd.) powders were used as the starting materials. The powders were simply mixed under ethanol using an agate mortar with the initial nominal composition; $Y_{0.73}B_{22}C_2$, which corresponds to the average refined composition in the previous reports.[10],[18] After drying, the powder mixtures were reactively sintered using an SPS machine (Dr. Sinter, Fuji Denpa Koki Co., Ltd.), as shown in **Fig. 1**.

For sintering, the mixtures were poured into a 10 mm diameter graphite die and pressed using graphite punches. A graphite paper was used as a release agent for ejecting the sample from the graphite die after sintering, and no BN was used. The sintering was carried out in a two-step process at the temperatures of T1 and T2. The mixtures were heated up to T1 of 1100–1300 °C in vacuum to remove volatile gases and B_2O_3 from surface oxidation of amorphous B, and then kept for 0–60 min in reduced N_2 gas atmosphere (−0.03 MPa) to introduce nitrogen into the mixtures. After that, they were heated up to T2 of 1650–1750 °C, and then kept for 0–10 min under a uniaxial pressure of ~30 MPa.

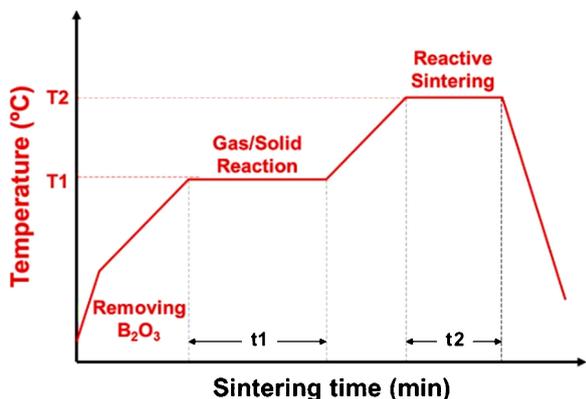† Corresponding author: T. Mori; E-mail: MORI.Takao@nims.go.jp

Fig. 1. The sintering schedule for synthesis of YB$_{22}$C$_2$N by reactive SPS.
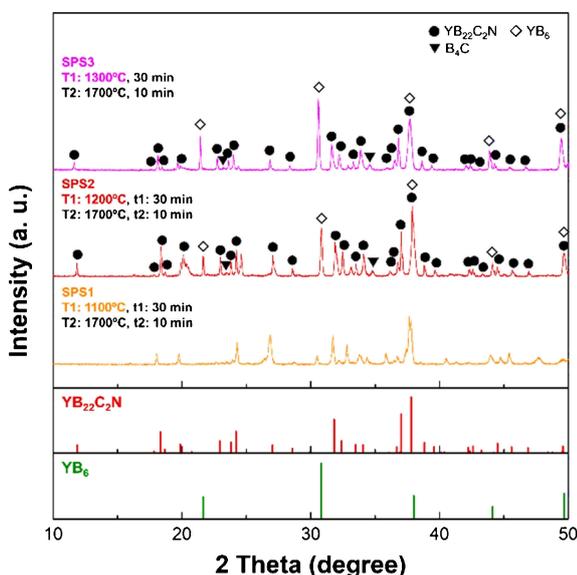

Fig. 2. The XRD patterns of the SPS1, SPS2 and SPS3 samples prepared with different nitrogen treatment temperature (T1) by reactive SPS.
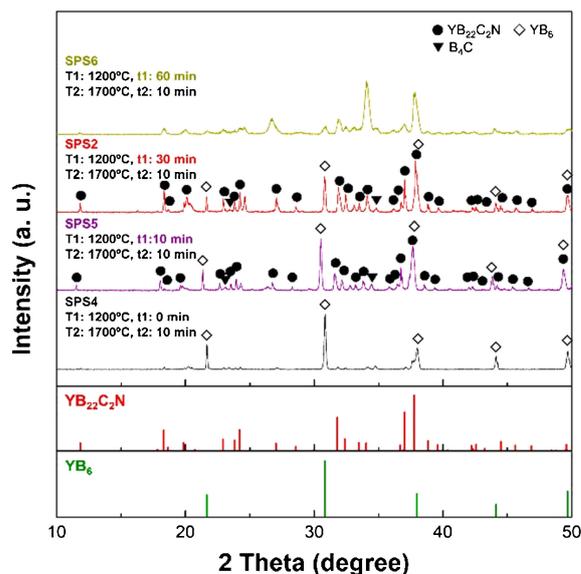

Fig. 3. The XRD patterns of the SPS4, SPS5, SPS2 and SPS6 samples prepared with different nitrogen treatment time (t1) by reactive SPS.

The constituent phases of the sintered samples were analyzed by X-ray diffraction (XRD, Smart lab 3, Rigaku) with Cu Kα radiation. The lattice parameters and the ratio of phases of the sintered samples were estimated by FullProf and PowderCell software, respectively. The electrical resistivities and Seebeck coefficients were evaluated in the temperature range of 100–500 °C using the standard 4-probe measurement setup of the ZEM-2 instrument (ADVANCE RIKO, Inc.).

Figure 2 shows the XRD patterns of the samples prepared at 1700 °C for 10 min by reactive SPS with different nitrogen treatment temperature (T1). The SPS1, SPS2 and SPS3 samples were kept at 1100, 1200 and 1300 °C for 30 min in N$_2$ gas atmosphere during heating, respectively. The YB$_{22}$C$_2$N phase was successfully synthesized when the samples were kept at 1200 or 1300 °C although they contained some amount of secondary phases including YB$_6$ and B$_4$C. The result implies that the N$_2$ gas/solid reaction is activated above 1200 °C.

The XRD pattern of the SPS3 sample showed a higher amount of YB$_6$ than the SPS2 sample. The transition from amorphous boron to crystalline α-rhombohedral boron occurs above 1300 °C.[22] It is thus considered that the reactivity among the YB$_4$ precursor, carbon and boron decreased when the mixture was kept at 1300 °C due to the transition of amorphous boron to crystalline boron, and hence less YB$_{22}$C$_2$N was formed. Furthermore, the reaction rate is closely related to the surface area. Therefore, the decrease of reactivity is also attributed to a decrease of the surface area of particles due to particle growth with increasing T1. Meanwhile, the formation of B$_4$C is attributed to not only the relatively low boron/carbon ratio originated from boron loss by evaporation of B$_2$O$_3$ occurred below T1,[10] but also carbon diffusion activated at high temperature during SPS due to its carbon-rich atmosphere.

Figure 3 shows the XRD patterns of the samples prepared at 1700 °C for 10 min by reactive SPS with different nitrogen treatment time (t1). In order to investigate the effect of the time on the gas/solid reaction, the SPS4, SPS5, SPS2 and SPS6 samples were kept at T1 for 0, 10, 30 and 60 min (t1) in N$_2$ gas atmosphere during heating, respectively. Here, 1200 °C was selected for T1 with considering the aforementioned results. When the mixture was heated up to the sintering temperature without holding at T1, the XRD pattern of the sample (SPS4) mainly exhibited strong peaks of YB$_6$ with very weak peaks of YB$_{22}$C$_2$N. The ratio of peaks of YB$_{22}$C$_2$N to YB$_6$ increased with increasing dwell time up to 30 min (SPS5 and SPS2). The results indicate that the gas/solid reaction step is beneficial for the synthesis of YB$_{22}$C$_2$N. Meanwhile, a dwell time exceeding 60 min (SPS6) at the gas/solid reaction step does not benefit for the synthesis of YB$_{22}$C$_2$N. Since the axial displacement of SPS6 sample continuously

**Table 1.** Lattice parameters and measured densities of the SPS2 and SPS5 samples prepared by reactive SPS

Sample	a (Å) (1 Å = 0.1 nm)	c (Å)	Density (g/cm^3)
SPS2	5.606(8)	44.750(6)	2.55
SPS5	5.601(2)	44.772(2)	2.79

changed during the gas/solid reaction step for 60 min although the nitrogen treatment was carried out at the isothermal temperature (Fig. S1), it is assumed that the deterioration is attributed to a reaction (or reactions) accompanying a volume change between amorphous boron and introduced nitrogen, which could be activated by the long treatment. Therefore, 30 min was selected as t1 for the N_2 gas/solid reaction step.

The estimated lattice parameters and measured densities of the SPS2 and SPS5 samples are given in the **Table 1**. The lattice parameters are well matched to those of the samples prepared at 1700 °C under 30 MPa by SPS in the previous study.[19] The measured densities of the samples consolidated by reactive SPS were also comparable to those of the samples prepared by conventional process with sintering additives, YB_4, YB_{25}(C), Si, SiC, Al and TiC,[19),20] even though no sintering additive available for densification was used. Since additives can often be detrimental to thermoelectric properties,[19),20] it indicates that reactive SPS has some advantages to densification of the bulk samples compared to the conventional process. However, since the present process involves volume changes attributed to several continuous reactions among starting materials, various shrinkage rates of multiple constituent phases and thermal expansion of graphite spacers, it is difficult to discuss on the densification behavior clearly. To investigate the reaction steps and densification behavior occurred during reactive SPS with gas/solid reaction technology, further study is required.

Next, the effect of the sintering temperature T2 on the reactive SPS for the synthesis of $YB_{22}C_2N$ was investigated. The SPS7, SPS2 and SPS8 samples were kept at 1200 °C for 30 min in N_2 gas atmosphere before subsequent heating, and then sintered at 1650, 1700 and 1750 °C for 10 min, respectively. All samples exhibited peaks of $YB_{22}C_2N$, as shown in **Fig. 4**. However, the $YB_{22}C_2N$ phase was decomposed when it was sintered above 1750 °C. Considering the densification during SPS, 1700 °C was selected as the temperature for the reactive sintering.

To determine the optimal sintering time t2 for the reactive SPS process, XRD measurements were carried out for the SPS9, SPS10 and SPS2 samples after sintering at 1700 °C for 0, 5 and 10 min, respectively (**Fig. 5**). For the SPS9 sample, which was heated up to 1700 °C and cooled down immediately without holding after the gas/solid reaction step, no peaks of $YB_{22}C_2N$ were identified. It implies that the gas/solid reaction step only helps introduce nitrogen into the mixture, and $YB_{22}C_2N$ is not synthesized during that step. The formation of the $YB_{22}C_2N$
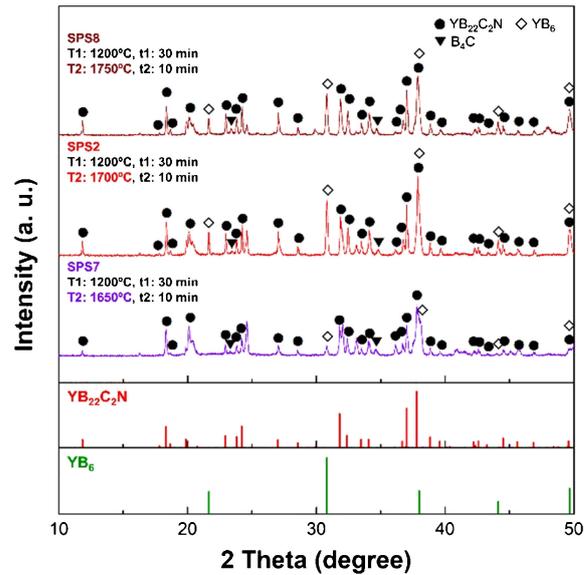
Fig. 4. The XRD patterns of the SPS7, SPS2 and SPS8 samples prepared with different sintering temperature (T2) by reactive SPS.
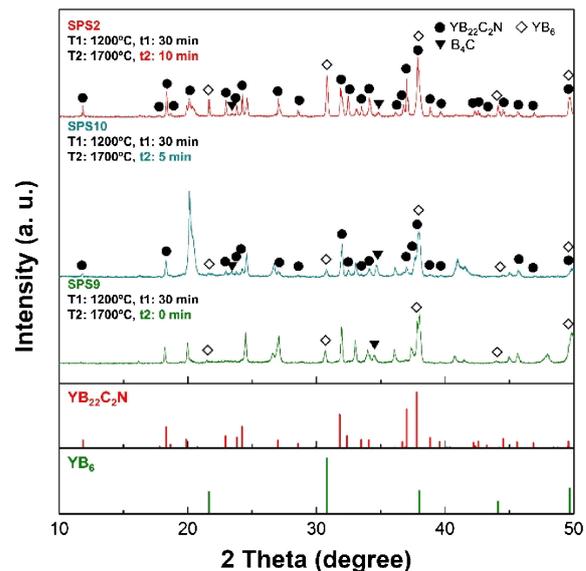
Fig. 5. The XRD patterns of the SPS9, SPS10 and SPS2 samples prepared with different sintering time (t2) by reactive SPS.

phase started when the sample was kept at 1700 °C for 5 min. The amount of the $YB_{22}C_2N$ phase increased when it was kept at 1700 °C for 10 min. Therefore, 10 min was selected as t2, which is the dwell time for the preparation of $YB_{22}C_2N$ by reactive SPS. Consequently, the SPS condition for the SPS2 sample was determined as the optimal condition for the synthesis of $YB_{22}C_2N$ via reactive SPS with gas/solid reaction in this study.

Figure 6(a) shows the ratio of $YB_{22}C_2N$, B_4C and YB_6 phases in the SPS2 and SPS5 samples. The result of quantitative analysis with approximation only considering these 3 phases seems to indicate that the SPS2 sample contains more amount of $YB_{22}C_2N$ and less amounts of secondary
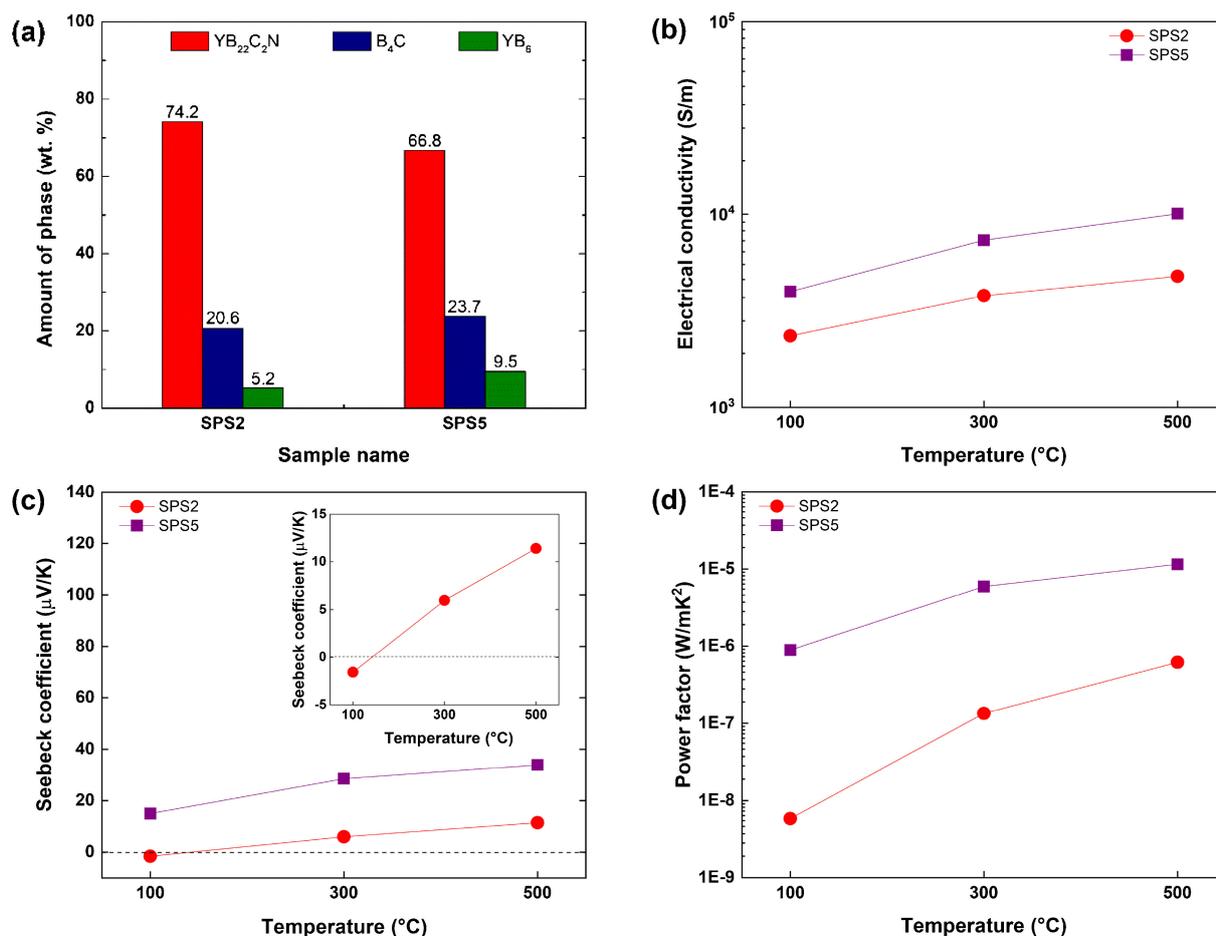
Fig. 6.   (a) The amount of YB$_{22}$C$_2$N, B$_4$C and YB$_6$ phases, (b) the electrical conductivities, (c) Seebeck coefficients and (d) the power factors of the SPS2 and SPS5 samples.

phases compared to the SPS5 sample. The temperature dependence of the thermoelectric properties of the SPS2 and SPS5 samples are plotted in Figs. 6(b)–6(d). As shown in Fig. 6(b), both samples exhibit semiconducting behavior in their electrical conductivities, which increase with increasing temperature. The SPS2 sample exhibited lower electrical conductivity values in all measured temperature range compared to those of the SPS5 sample. The lower electrical conductivity is attributed to less amount of electrically conductive secondary phases, B$_4$C and YB$_6$, and its lower density.

The measured Seebeck coefficient values are shown in Fig. 6(c). At 100 °C, the SPS5 sample exhibited a positive value, whereas the SPS2 sample exhibited a negative value. The SPS2 sample shows a general shift toward n-type behavior over the whole temperature region. It indicates that the thermoelectric behavior of the sintered sample is changed from p-type to n-type with increasing amount of YB$_{22}$C$_2$N, which is known as an n-type material.[15),16),18)] The Seebeck coefficient of SPS2 sample was changed from negative to positive value between 100 and 300 °C, and then increased with increasing temperature. It is considered that the increase of positive Seebeck coefficients with the temperature are attributed to the presence of B$_4$C.[9),17),23)] Small amounts of B$_4$C secondary

phase have been previously shown to shift this type of material from n-type behavior to p-type behavior.[15),17)] Figure 6(d) shows the temperature dependence of power factors of each sample. The amount of B$_4$C could be reduced by controlling boron/carbon ratios in the synthesis.[10)] Through developing an initial composition containing the optimal boron/carbon ratio and reducing the effect of carbon-rich atmosphere with using BN as the release agent instead of the graphite paper, improvements of the absolute value of the negative Seebeck coefficient and power factor are expected.

In this study, a new synthesis route for preparation of polycrystalline YB$_{22}$C$_2$N by reactive SPS was developed. N$_2$ gas/solid reaction technology carried out at 1200 °C for 30 min during SPS effectively helped the formation of the objective phase. The most homogeneous YB$_{22}$C$_2$N was synthesized when it was sintered at 1700 °C for 10 min after the gas/solid reaction step, and it exhibited n-type thermoelectric behavior at low temperature. Consequently, by developing the present synthesis method, the total process steps and the whole process time required to synthesize YB$_{22}$C$_2$N were dramatically shortened from ≥9 to only 3 steps, and from ≥4 days to only ~3 h, respectively. This new method is expected to open the door for more effective synthesis of complex borocarbonitrides.

References

1) B. T. Matthias, T. H. Geballe, K. Andres, E. Corenzwit, G. W. Hull and J. P. Maita, *Science*, **159**, 530 (1968).

2) K. H. J. Buschow, "Boron and Refractory Borides", Ed. by V. I. Matkovich, G. V. Samsonov, P. Hagenmuller and T. Lundstrøm, Springer, Berlin (1977) pp. 494–515.

3) J. Etourneau and P. Hagenmuller, *Philos. Mag. B*, **52**, 589–610 (1985).

4) R. J. Cava, H. Takagi, H. W. Zandbergen, J. J. Krajewski, W. F. Peck, Jr., T. Siegrist, B. Batlogg, R. B. Van Dover, R. J. Felder, K. Mizuhashi, J. O. Lee, H. Eisaki and S. Uchida, *Nature*, **367**, 252–253 (1994).

5) T. Mori, "Handbook on the Physics and Chemistry of Rare Earths", Ed. by K. A. Gschneidner, Jr., J.-C. G. Bünzli and V. K. Pecharsky, Elsevier, Amsterdam (2008) pp. 105–173.

6) D. J. Kim, J. Xia and Z. Fisk, *Nat. Mater.*, **13**, 466–470 (2014).

7) A. Koitzsch, N. Heming, M. Knupfer, B. Büchner, P. Y. Portnichenko, A. V. Dukhnenko, N. Y. Shitsevalova, V. B. Filipov, L. L. Lev, V. N. Strocov, J. Ollivier and D. S. Inosov, *Nat. Commun.*, **7**, 10876 (2016).

8) N. E. Sluchanko, A. N. Azarevich, M. A. Anisimov, A. V. Bogach, S. Y. Gavrilkin, M. I. Gilmanov, V. V. Glushkov, S. V. Demishev, A. L. Khoroshilov, A. V. Dukhnenko, K. V. Mitsen, N. Y. Shitsevalova, V. B. Filippov, V. V. Voronov and K. Flachbart, *Phys. Rev. B*, 93, 085130 (2016).

9) T. Mori, *J. Solid State Chem.*, **275**, 70–82 (2019).

10) F. Zhang, A. Leithe-Jasper, J. Xu, T. Mori, Y. Matsui, T. Tanaka and S. Okada, *J. Solid State Chem.*, **159**, 174–180 (2001).

11) F. Zhang, F. Xu, A. Leithe-Jasper, T. Mori, T. Tanaka, J. Xu, A. Sato, Y. Bando and Y. Matsui, *Inorg. Chem.*, **40**, 6948–6951 (2001).

12) T. Mori and A. Leithe-Jasper, *Phys. Rev. B*, **66**, 214419 (2002).

13) T. Mori and H. Mamiya, *Phys. Rev. B*, **68**, 214422 (2003).

14) T. Mori, R. Sahara, Y. Kawazoe, K. Yubuta, T. Shishido and Y. Grin, *J. Appl. Phys.*, **113**, 17E156 (2013).

15) T. Mori and T. Nishimura, *J. Solid State Chem.*, **179**, 2908–2915 (2006).

16) T. Mori, T. Nishimura, K. Yamaura and E. Takayama-Muromachi, *J. Appl. Phys.*, **101**, 093714 (2007).

17) T. Mori, T. Nishimura, W. Schnelle, U. Burkhardt and Y. Grin, *Dalton T.*, **43**, 15048–15054 (2014).

18) O. Sologub and T. Mori, *J. Phys. Chem. Solids*, **74**, 1109–1114 (2013).

19) D. Berthebaud, T. Nishimura and T. Mori, *J. Mater. Res.*, **25**, 665–669 (2010).

20) D. Berthebaud, T. Nishimura and T. Mori, *J. Electron. Mater.*, **40**, 682–686 (2011).

21) T. Borkar, S. Nag, Y. Ren, J. Tiley and R. Banerjee, *J. Alloy. Compd.*, **617**, 933–945 (2014).

22) T. Machaladze, M. Samkharadze, N. Kakhidze and M. Makhviladze, *Open J. Inorg. Chem.*, **4**, 18–20 (2014).

23) C. Wood and D. Emin, *Phys. Rev. B*, **29**, 4582–4587 (1984).